Journal Name

COMMUNICATION

1cm^2 $CH_3NH_3PbI_3$ mesoporous solar cells with 17.8% steady-state efficiency by tailoring front FTO electrodes

Received 00th January 20xx,
Accepted 00th January 20xx

DOI: 10.1039/x0xx00000x

www.rsc.org/

Mohammad Afzaal,*[a] Heather M. Yates,[a] Arnaud Walter,[b] Sylvain Nicolay,[b] and Christophe Ballif,[b]

In this article, we investigate the effects of atmospheric-pressure chemical vapour deposited fluorine doped tin oxide (FTO) thin films as front electrodes for the fabrication of mesoporous perovskite solar cells with an active area of 1cm^2 and compare with use of a commonly used commercial transparent conducting oxide. The effects of sheet resistance (*Rs)* and surface roughness are both closely linked to the film thickness. In order to separate out these effects the characteristics of the deposited FTOs were carefully controlled by changing the fluorine doping levels and the number of passes under the coating head to give films of specific thicknesses or *Rs*. Under AM 1.5 sun illumination and maximum power point tracking, the optimised FTOs yielded a steady-state power conversion efficiency of 17.8%, higher than that of the reference cell fabricated from the commercial FTO. We attribute the improved cell efficiency to increased fill factor and a lower series resistance resulting from the lower *Rs* and increased thickness of these FTO substrates. This low-cost and viable methodology is the first such type of study looking independently at the significance of FTO roughness and resistance for highly efficient mesoporous perovskite solar cells.

The quest for low-cost and high-efficiency solar cells has provided much impetus towards earth abundant materials and efficient fabrication processes. This is particularly true for the organic-inorganic perovskite solar cells (PSCs) with reported efficiencies in excess of 22%.[1] The PSCs generally consist of a counter electrode/hole transporting layer/perovskite/electron transport layer supported on a transparent conducting oxide (TCO) coated glass.[2] In the mesoscopic form, the perovskite (PVK) sensitizer is infiltrated through a mesoporous metal oxide scaffold such as titanium dioxide (TiO_2) to facilitate a large surface active area. For the planar structures, no scaffold is required and can be described having either n-i-p or p-i-n geometry (depending on the charge collection direction).[3]

Attempts to boost power conversion efficiencies (PCEs) in PSCs have mainly concentrated on tailoring and improving the PVK geometries,[4] associated film deposition processes,[5] and transport layers.[6] One common feature of nearly all the work to date is the choice of commercial TCOs, in particular fluorine doped tin oxides (FTOs) namely the TCO22-15 (Solaronix) or TEC A7 (NSG). These commercial samples have excellent transmission and low *Rs*, along with rough scattering surfaces in the case of TEC 7 which is desirable for silicon-based solar cells. Silicon being a poor light absorber, rough FTOs with high root mean squared values (RMS) are needed to increase the optical path length of incident light at the interface. The effect has been previously demonstrated in micromorph tandem cells by the authors.[7] On the contrary, the PSCs exhibit a large optical absorption coefficient along with an excellent exciton diffusion length and charge-carrier mobility.[8] To facilitate the maximum absorption of light by the PVK layer, smoother FTO surfaces with low optical haze *i.e.* reduced scattering are desired, without compromising the electron mobility. This enables the formation of uniform and pinhole free electron blocking layers which will promote the charge separation and minimise electron-hole recombination. In a recent study, we have shown the need for smooth FTO surfaces with low *Rs* to aid deposition of pin-hole free blocking layers and well adhered PVK layers for high performance PSCs.[9] To emphasis the point, Tavakoli and co-workers have exhibited improved PCEs in the region of 8% for planar PVK solar cells, after ion milling the FTOs for 10 minutes to achieve smooth surfaces.[10] Without this treatment, a PCE of 6.6% was reported. Park et al concluded that smooth electron transporting layers are essential to increase the light absorption and improve physical contact with the PVK layers.[2]

The *Rs* and surface roughness of atmospheric-pressure chemical vapour deposition (APCVD) deposited FTOs are strongly linked to the film thickness. These properties in turn affect the overall efficiency of solar cells. For example, a

[a] *Materials and Physics Research Centre, University of Salford, Manchester, M5 4WT, United Kingdom. E-mail: M.Afzaal@salford.ac.uk*
[b] *Centre Suisse d'Electronique et de Microtechnique (CSEM), PV-Center, Jaquet-Droz 1, 2002 Neuchâtel, Switzerland*

Electronic Supplementary Information (ESI) available: Deposition of thin films, fabrication of solar cells, characterisation of thin films, cell characterisation, grain sizes and texture coefficients of selected films, AFM images, photovoltaic parameters of the solar cells processed with commercial and batch 2 FTOs. See DOI: 10.1039/x0xx00000x

thicker film will have the advantages of lower *Rs* hence increasing efficiency of transporting the generated current and a higher roughness which could increase the light scattering so increasing the efficiency in light used (although this is a relatively minor factor for PSC's). In addition, the rougher FTO surface could lead to a greater surface contact area between itself and the blocking layer, and hence perovskite absorber. Conversely, a thicker layer has the disadvantages of increased light absorption, so less light reaching the absorber. Also the FTO roughness can lead to the development of a poorer interface with the blocking layer and hence perovskite, together with increased likelihood of pinholes and hence shunted cells.

Continuing our efforts to identify optimum FTO properties for high performance PSCs with an active area of 1cm^2, we attempt to separate the effects of thickness (roughness) and *Rs*. We explore the use of FTOs with same *Rs* with different thicknesses (marked as S1-S3 in batch 1) and similar thicknesses having a range of *Rs* (marked as S4-S6 in batch 2) and show how they might impact PCEs of PSCs. To produce samples ($\times$ 3) of similar properties under different conditions, fluorine doping levels and number of deposition passes of the coated head were adjusted in an APCVD process as described in supplementary information.[11] A summary of conditions is given in Table 1. A comparison with PSCs fabricated using a commercial FTO (Solaronix TCO22-15) is also provided to highlight the potential of deposited FTOs.

The X-ray powder diffraction (XRPD) studies confirmed the deposition of tetragonal SnO_2 films, without any impurities (Figure 1). One notable difference is the degree of preferred orientation which according to the texture coefficient (TC) calculations is higher for S1 along the (200) direction (Table S1). In general, FTO films with a strong preferred orientation along the (200) axis are desired due to favourable electrical conductivities arising from the absence of Sn^{2+} trap states.[12] According to Scherrer's equation, S1 and S7 (batch 3 with low *Rs* and reduced carrier concentration (*N*)) have significantly large crystallite sizes (≈ 37 nm) compared to reference FTO (≈ 26 nm) as listed in Table S1. Crystallite size changes are mirrored in the different surface morphologies evidented in the corresponding scanning electron microscope (SEM) images (Figure 1). Sample S1 consists of pyramidal features with clear textured grain boundaries, also reflected in TC calculations. The dense morphology of S7 consists of compact randomly orientated features whereas the reference FTO has a predominantly granular structure.

As evident in Table 1, batch 1 (S1-S3) samples have similar *Rs* (≈ 9 Ω/□) with film thicknesses ranging between ≈ 0.51 – 0.98 µm. This is achieved by increasing the dopant concentration, trifluoroacetic acid (TFAA) in water from 0.3 to 1 M and decreasing the number of passes simultaneously under the coating head. As the doping levels only change the *Rs*, different number of passes are required to modify the film thicknesses and their resistivities. The batch 2 (S4-S6) samples are produced with reduced number of passes resulting thinner films with increased *Rs*. One net result is the reduced mobility (μ) (below 20 cm^2/Vs) and increased *N* (5.2 – 7.8 $\times$ 10^{20} cm^{-3}) properties compared with batch 1 samples (μ = 26 – 31 cm^2/Vs, *N* = 2.3 – 4.3 $\times$ 10^{20} cm^{-3}). For Solaronix TCO22-15, μ = 28 cm^2/Vs and *N* = 4.2 $\times$ 10^{20} cm^{-3} as determined by us.[9]

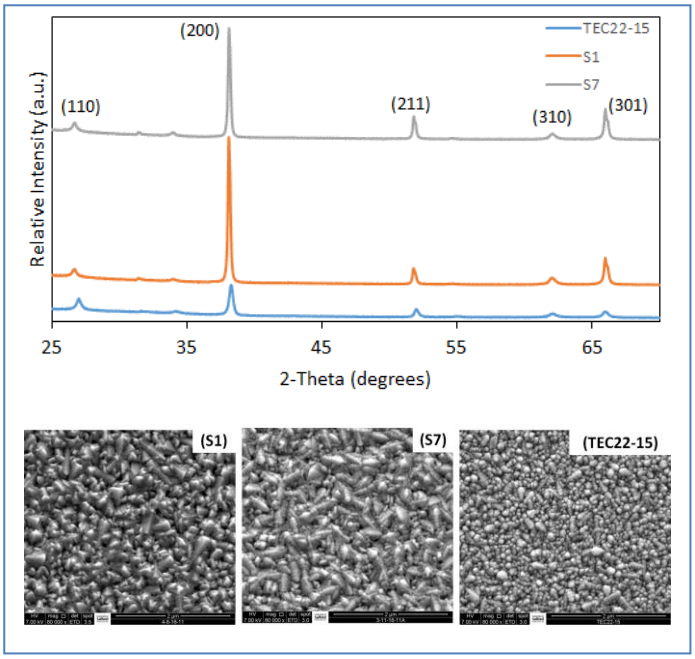

Fig. 1 (Top) XRD patterns and (Bottom) SEM images of FTO coatings carried out under different deposition conditions. (Scale = 2 µm)

Mean reflectance (*R*) and transmittance (*T*) properties of FTOs are strongly thickness-dependent and remain unaffected by the doping levels as also previous seen (Figure 2).[13] To illustrate the point, increasing film thicknesses in batch 1 decreased *R* and *T* values (between 400 – 1100 nm) and are in-line with a previous study on FTO films.[14] The increased thickness leads to more adsorption of light and hence lower *T*, despite the decreased level of doping which would generally be expected to lead to reduced absorption (for a fixed film thickness). However, we would usually expect a corresponding increase in *R*, which does not occur. This is likely to be due to the increased loss of light *via* optical scattering from the thicker and hence rougher surfaces, as seen in Figure 2. The change in thickness can be seen particularly clearly in the *R* spectra with the shortening of the interference fringe oscillation period with increasing thickness. In contrast, when having different *Rs* but of same thickness, S4 – S6 in batch 2 have similar *R* (≈ 9 %) and *T* (≈ 88± 1%) with the slightly thinner sample having the slightly higher *T*. Batch 1 samples showed greater attenuation of the lower wavelength values in the spectra than those of Batch 2, which is caused by their greater roughness, as seen via optical haze measurements. This is confirmed by the greater RMS values (≈ 25 nm) of resulting atomic force microscopy (AFM) images given in Figure S1.

To validate our T values, measurements performed on TCO22-15 give an average of 80 % which is in-line with the reported value,[15] particularly as our measurements are done at 30° (due to the geometry of the instrument) rather than 90°

so slightly reduce T and increase R. The optical haze is dependent on film thickness and surface roughness.[16] For example, the higher haze in batch 1 is due to their greater thickness than batch 2 (Figure 2). Similarly, a large variation in haze between samples from batch 1 is thickness-dependent,

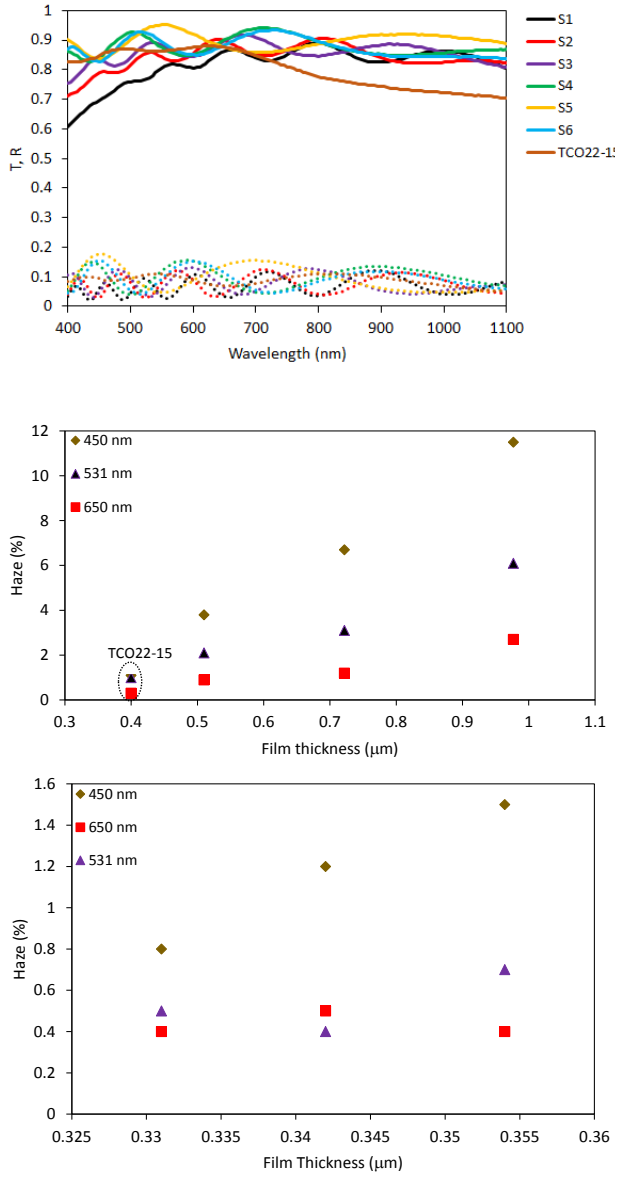

while batch 2 shows much less variation as closer in thickness.

Fig. 2 (Top) Transmission (solid lines) and reflection (dotted lines) spectrum of deposited and commercial FTOs. (Middle) and (bottom) haze values as a function of film thicknesses for batch 1 and 2, respectively.

The average *T* for the reference FTO is lower than that of the APCVD samples, due mainly to its decided reduction at > 750 nm. The period of interference oscillation is as would be expected for its film thickness, slightly shorter than Batch 2 and longer than Batch 1. Interestingly the interference amplitude is much smaller than that of our samples, suggesting that its average refractive index is different. This could relate to the film density or the thin silica barrier layer between glass and FTO layer.[17] Values for optical haze and average reflection are in-line with the APCVD results when thickness is taken into consideration as can be seen in figure 2.

We fabricated 1cm^2 active mesoscopic PSCs on deposited and commercial FTOs and the device statistics are shown in Figures 3 and S2. Sputtered hole blocking TiO_{2-x} and spin-coated perovskite layers are in the order of 20 nm and 300 nm, respectively. After sintering of the TiO_2 paste to yield a charge conducting mesoporous structure (thickness 150nm), spin coated absorber $CH_3NH_3PbI_3$ (thickness = 300 nm) followed by 180 nm thick hole transporting Spiro-OMeTAD layers are deposited. The devices are finally completed with 100 nm thermally evaporated gold layers.

In batch 1 cells (constant R_s), clear trends were seen with changes to FTO thickness and hence roughness. Increasing FTO thickness reduced open circuit voltage (*Voc*) and current density, (*Jsc*) while improving fill factor (*FF*), which is the over-ridding factor in gaining the higher efficiencies. The reduction in *Jsc* is due to the higher absorption for these thicker films. Power conversion efficiencies (PCEs) as high as 16% was seen for one set of the samples, greater than that seen for the cell from the commercial reference. For batch 2 samples (constant thickness), the trends against *Rs* were less clear. There was possibly an issue with sample S4 due to the perovskite processing which led to its final lower efficiency. However, as *Rs* increased there was an increase in *Jsc* and *Voc*, with a corresponding decrease in in *FF* and hence efficiency. Also shown in Figure S2, the *Rs* variation directly impacts on the series resistance (*Roc*) with S6 (low *Rs*) exhibiting reduced *Roc*. This has a direct effect on the *FF* in that it is higher for TCO's with lower *Rs*. On the other hand, a higher *Rs* comes with a reduced absorptance that in turn impacts *Jsc*. As a matter of fact, cells with the more resistive FTO exhibit the higher *Jsc*. There is no obvious link between the maximum power point tracking (MPPT) of cells and FTO film resistivities, due to issues with the deposition of absorber layer in the case of S4 as mentioned above (Fig S3). It is also worth pointing out here that any processing changes during the deposition of FTOs would alter film properties in particular *T*, film roughness and roughness and subsequently inluenc PCEs of solar cells.

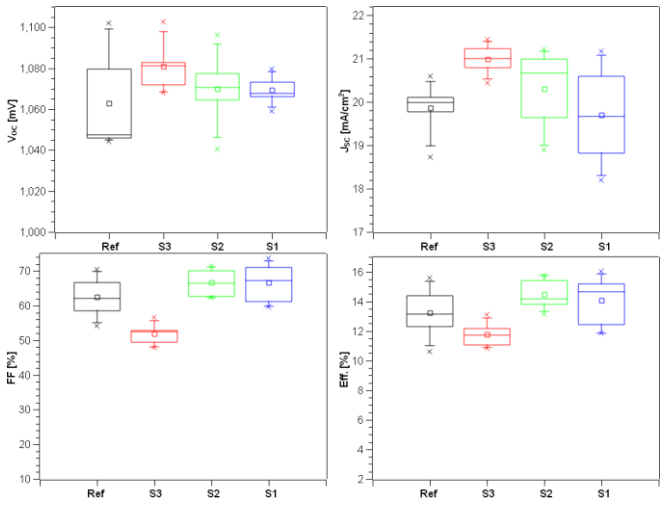

Fig. 3 Statistical analysis of the photovoltaic parameters of the solar cells processed with batch 1 FTOs.

Based on the results in Batches 1 and 2, a 3rd batch of samples was produced concentrating on low *Rs* and reduced *N*. In batch 3, several thick FTOs of similar properties were deposited with *Rs* ~ 7 Ω/□, moderate μ and reduced *N*. Typical sample information is provided in table 1. These were relatively thick FTOs with increased haze, but without sacrificing the optical transmission which is higher than that of reference FTO (Figure 3). The increased roughness (RMS = ~ 26 nm) of Batch 3 (Figure S1) samples over that of the reference FTO (RMS = ~ 14 nm) can be inferred from its much greater optical haze, as shown in Figure 4. The determined *T* and *R* for batch 3 are ~ 83 % and 8 %, respectively.

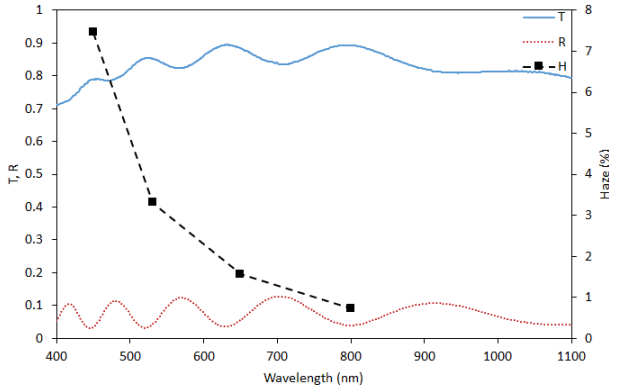

Fig. 4 Transmission, reflection and haze values for batch 3.

To test reproducibility a number of devices were prepared using batch 3 FTOs. These consistently showed good, closely grouped cell properties and hence excellent PCEs with values averaging 16.3 ± 1.27 % (Figure S4). Current-voltage hysteresis (forward and back scans) and MPPT scans of the champion device are demonstrated in Figure 5. Despite showing a small hysteresis, high PCE of 17.8% under MPPT is obtained. This is an improvement from the reported values for the $CH_3NH_3PbI_3$ system. For example, Lee and co-workers reported PCE of 16.6 % on 0.16 cm^2 active area of the device.[18] By a different group, a PCE of 14.3 % is seen for the best performing device.[19] It is also worth pointing out here that efficiencies greater than 17.8 % are seen for mixed halide perovskites[20,21] and so a direct comparison cannot be made with studied non-mixed halide system.

The observed steady-state efficiency in our champion data is predominantly due to an improved *FF* of 77.5% driven by the low *Roc* of the cells as shown in Table 2. After integrating the external quantum efficiency (EQE) curve of the device, J_{sc} was found to be 20.88 mA/cm^2 which is consistent with the measured J_{SC} determined by J-V measurements. This ensures the accuracy of the device J-V measurements. The observed steay-state efficiency is improvement from the reported values for the similar $CH_3NH_3PbI_3$.

The above findings indicate that a single FTO property for example, having low *Rs* alone does not influence PCEs. A correct combination of thickness dependent μ and *N*, and surface related transmission and haze are required to make significant contribution towards PCEs. Due to various competing properties, a balance is needed between required properties. This is evident for thicker batch 3 samples having a higher transmission than Batch 1 and greater haze than the reference TCO, without the loss of μ (as occurs for Batch 2). The overall result is increased PCEs through improved FF and reduced *Roc*. Currently, studies are underway to extend the potential of tailor-made FTOs for large area planar PVK cells which will be reported elsewhere.

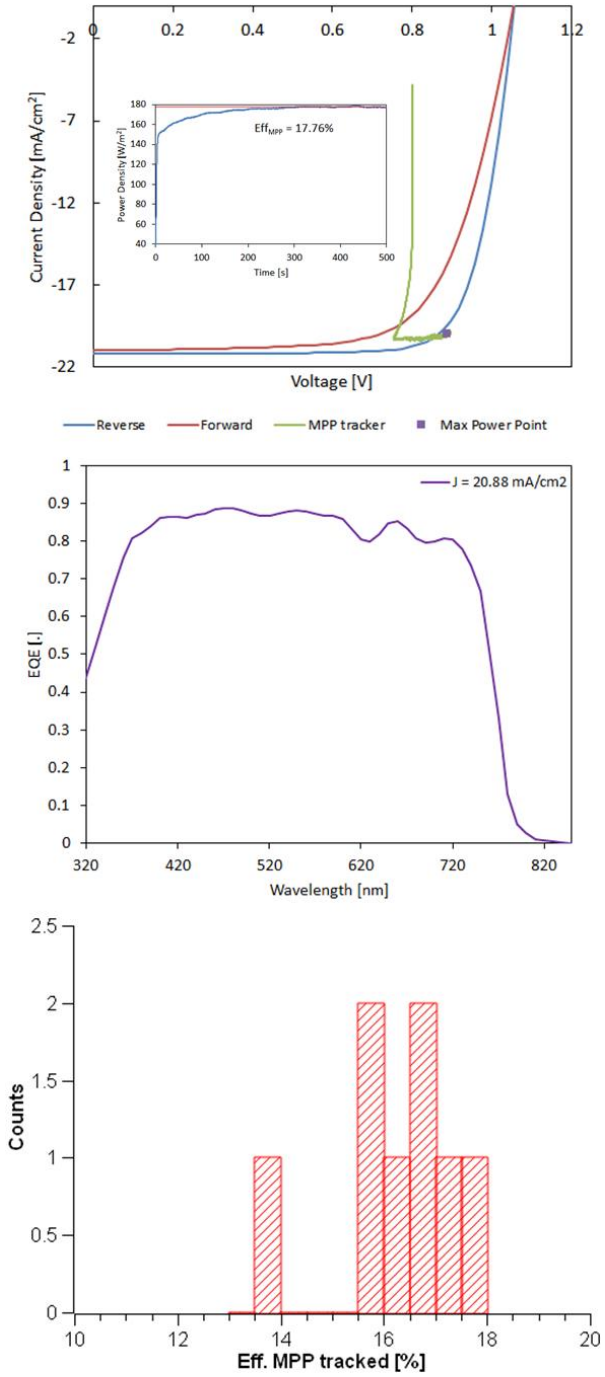

Fig. 5 (Top) Photocurrent-voltage curve under forward and reverse scan direction measured at a simulated AM1.5 sun illumination and maximum power point tracking of champion device. (Middle) corresponding external quatum efficiency

spectrum. (Bottom) Resulting power conversion efficiencies of solar cells using batch 3 FTOs through maximum power point tracking.

Conclusions

We have successfully shown that combined sheet resistance, transmission, haze and mobility FTO properties could yield steady-state efficiency values of 17.8 % for 1cm^2 mesoporous PSCs. This improvement was a result of high fill factor driven by low series resistance. Careful adjustment of fluorine doping levels and thicknesses in an industrial scalable atmospheric-pressure CVD process resulted in FTO films with a range of properties. This work aims to highlight the importance of front electrodes as a mean of achieving of stabilised efficiencies and could be extended to planar PSCs.

Acknowledgements

This work was financed by Framework 7 grant FP7 NMP.2012.1.4-1 309530 PLIANT "Process line implementation for applied surface nanotechnologies".

References

1 www.nrel.gov/ncpv/images/efficiency_chart.jpg Accessed 24.11.2016.
2 J. Choi, S. Song, M. T. Hörantner, H. J. Snaith and T. Park, *ACS Nano*, **2016**, *10*, 6029–6036.
3 C. Zuo, H. J. Bolink, H. Han, J. Huang, D. Cahen and L. Ding, *Adv. Sci*., **2016**, *3*, 1500324.
4 N. G. Park, *Mater. Today* **2015**, *18*, 65−72.
5 Y. Chen, M. He, J. Peng, Y. Sun and Z. Liang, *Adv. Sci.,* **2016**, *3*, 1500392.
6 (a): G. Yang, H. Tao, P. Qin, W. Ke and G. Fang, *J. Mater. Chem. A*. **2016**, *4*, 3970-3990. (b): Z. Yu and L. Sun, *Adv. Energy Mat.*, **2015**, *5*, 1500213.
7 H. M. Yates, P. Evans, D. W. Sheel, S. Nicolay, L. Ding and C. Ballif, *Surf. Coat Technol*. **2013**, *230*, 228-233.
8 M. A. Green, A. Ho-Baillie and H. J. Snaith, *Nat. Photonics*, **2014**, *8*, 506-514.
9 H. M. Yates, M. Afzaal, A. Walter, J. L. Hodgkinson, S. J. Moon, D. Sacchetto, M. Bräuninger, B. Niesen, S. Nicolay, M. McCarthy, M. E. Pemble, I. M. Povey and C. Ballif, *J. Mater. Chem. C* **2016**, *4*, 11269-11277.
10 M. M. Tavakoli, L. Gu, Y. Gao, C. Reckmeier, J. He, A. L. Rogach, Y. Yao and Z. Fan, *Sci. Rep.*, **2015**, *5*, 14083.
11 M. Afzaal, H. M. Yates and J. L. Hodgkinson, *Coatings,* **2016**, *6*, 43.
12 M. Soliman, M. M. Hussein, S. El-Atawy and M. El-Gamal, *Renew. Energy*, **2001**, *23*, 463-470.
13 F. Arefi-Khonsari, N. Bauduin, F. Donsanti and J. Amouroux, *Thin Solid Films,* **2003**, *427*, 208-214.
14 N. Noor, C. K. T. Chew, D. S. Bhachu, M. R. Waugh, C. Carmalt and I. P. Parkin, *J. Mater. Chem. C* **2015**, *3*, 9359-9368.
15 http://shop.solaronix.com/tco22-15.html
16 R. Otsuka, T. Endo, T. Takano, S. Takemura, R. Murakami, R. Muramoto, J. Madarász, and M. Okuya, *Jpn. J. Appl. Phys.,* **2015**, *54*, 08KF03.
17 Personal communication.
18 Y. H. Lee, J. Luo, R. Humphry-Baker, P. Gao, M. Gratzel and M. K. Nazeeruddin, *Adv. Funct. Mater*., **2015**, *25*, 3925-3933.
19 H. Wang, Y. Rahaq and V. Kumar, *Sci. Rep.*, **2016**, *6*, 29567.
20 X. Li, D. Bi, C. Yi, J.-D. Decoppet, J. Luo, S. M. Zakeeruddin, A. Hagfeldt and M. Gratzel, *Scien*ce 2016, **353**, 58-62.
21 W. S. Yang, J. H. Yoh, N. J. Jeon, Y. C. Kim, S. Ryu, J. Seo and S. I. Seok, *Science* 2015, **348**, 1234-1237.

Journal Name

COMMUNICATION

Table 1 Summary of Growth Parameters and Properties of Thin Films at 600 °C with Sn/H_2O Ratio Fixed at 1:5

	Sample	TFAA Concentration (M)	*Rs* (Ω/□)	*d* (μm)	$p/\times10^{-4}$ (Ω.cm)	μ (cm^2/Vs)	$N/\times10^{20}$ (cm^{-3})
Batch 1	S1	0.3	8.7	0.977 (± 0.018)	8.5	28	2.3
	S2	0.8	8.8	0.722 (± 0.007)	6.35	26	4.1
	S3	1	9.1	0.51 (± 0.014)	4.64	31	4.3
Batch 2	S4	0.6	20.8	0.342 (± 0.012)	7.12	19	5.4
	S5	0.8	29.6	0.331 (± 0.014)	9.80	15	5.2
	S6	1	14	0.354 (± 0.01)	4.96	20	7.8
Batch 3	S7	1	7.2	0.828 (± 0.009)	5.96	30	3.7
	Ref*	N/A	13	0.400	5.2	28	4.2

* refers to Solaronix TCO22-15.[15] *Rs*: sheet resistance, *d*: film thickness, *p*: resistivity, μ: mobility, *N*: carrier concentration

Table 2. Photovoltaic parameters of chamption device with 1cm^2 active area

Scan direction	Voc [mV]	Jsc [mA/cm^2]	FF [%]	Eff. [%]	Roc [Ω.cm^2]	Rsc [Ω.cm^2]	Eff. MPP [%]
Reverse	1055.70	21.19	77.52	17.34	4.86	150908.90	17.8
Forward	1053.62	21.00	68.19	15.09	8.00	3117.97	